Appendix to Results

Regression analysis of the ASM mass increment as a function of increased myocyte proliferation and decreased apoptosis.

Inter-group comparisons showed increased ASM mass, increased numbers of $PCNA^+$ and decreased numbers of $TUNEL^+$ ASM cells in the recipients of $CD4^+$ T cells upon repeated antigen challenge. To further explore statistically these effects we performed regression analysis. First we analyzed the relationship between proliferation and apoptosis. There was no significant association between proliferation and apoptosis within the control groups ($P \geq 0.13$ for both the epithelium and the ASM in the OVA/BSA and Sham/OVA groups). In the OVA/OVA group, antigen challenge induced an inverse non-linear relationship between proliferation and apoptosis in both the airway epithelium (hyperbolic, R= -0.52, $P=0.009$) and the ASM (exponential, R= -0.61, $P=0.002$), suggesting that the balance between proliferation and apoptosis in those structural cell types is altered in airway remodeling (Figure S1 A-B). These data suggest that, if the balance that determines normal tissue turnover (control animals) is altered in airway remodeling, proliferation and apoptosis might then be cross-regulated. A strong positive linear association seen between the counts in airway epithelium *versus* ASM for $PCNA^+$ cells/mm^2 (R=0.87, $P<0.001$) and $TUNEL^+$ cells/mm^2 (R=0.77, $P<0.001$) (Figure S1 C-D) suggests a concomitant response of both structures to locally delivered signals. Next we modeled the effect of the changes in apoptosis and proliferation on ASM mass. We observed a significant inverse association between apoptosis and ASM mass (hyperbolic, R= -0.77, $P<0.0001$) (Figure S1 E), where the decrease in apoptosis accounts statistically for 59% of the observed change in ASM mass ($R^2=0.589$). Conversely, we found a weak association between myocyte proliferation and ASM mass (R=0.41, $P=0.049$) (Figure S1 F), where the increase in

myocyte proliferation could statistically explain 16% of the change in ASM mass (R^2=0.165). The modeling of the variation in ASM mass as a combined result of regulation of myocyte proliferation and apoptosis suggests therefore that the inhibition of apoptosis accounts for the increase in ASM mass to a larger extent than the increase in proliferation. Part of the approximately 25% unexplained variability of ASM mass may be attributable to hypertrophy.

Appendix to Methods

Preparation of primary rat ASM cell cultures.

OVA-sensitized BN rats were sacrificed with an overdose of sodium pentobarbital and their tracheae, main bronchi and lobar bronchi were excised. After removing visible fascia and cutting the tracheae longitudinally, the tissue was washed in HBSS and digested with 0.2% collagenase IV (6 mg collagenase per trachea) and 0.05% elastase IV (0.75 mg elastase per trachea) (Sigma) in HBSS for 30 min at 37° C, with mild agitation. The supernatant from the digestions was then decanted into a new tube and centrifuged at 500·*g* for 6 min, and the pellet containing ASM cells was re-suspended in 1:1 DMEM:Ham's F12 with 10% FBS, 2mM glutamine, 100 U/ml penicillin and 100 μg/ml streptomycin. The cell suspension was then plated onto 35-mm cell culture dishes, the cultures washed with PBS 24 h later and the medium replaced. The ASM cell cultures were grown to subconfluence, trypsinized, and subcultured onto 6-well cell culture plates for the co-culture assay.

Figure S1

Regression analysis. The relationship between proliferation and apoptosis in airway epithelium (**A**) and ASM (**B**) suggests cross-regulation. The regression trends suggest that the induction of cell proliferation may have a higher threshold than the prolongation of survival. Panel B corresponds to the ASM TUNEL^{+} versus PCNA^{+} cells/mm2 projection in the 3D model shown in (G) and Figure 6A. The association between airway epithelium and ASM frequencies for proliferation (**C**) and apoptosis (**D**) suggests an epithelial-mesenchymal concomitant response. (**E**) Statistically, the growth of ASM results to a larger extent from inhibition of apoptosis, which accounts for approximately 59% of the increase. The inverse relationship between ASM mass and apoptosis becomes linear and closely correlated in the OVA/OVA group. On the contrary, myocyte proliferation is a weak predictor of ASM mass (**F**). Panels (E) and (F) correspond to the respective 3-D projections in (G) and Figure 6A. The legend inset in (A) applies to all A-F panels. (**G**) Tri-variable arrangement of ASM mass (x10^{-3}) *versus* TUNEL^{+} cells/mm^2, ASM mass (x10^{-3}) *versus* PCNA^{+} cells/mm^2, and TUNEL *versus* PCNA cells/mm^2 functions. The 3-D multivariable function in Figure 6A was built from the regression curve projections shown here.

Figure S1

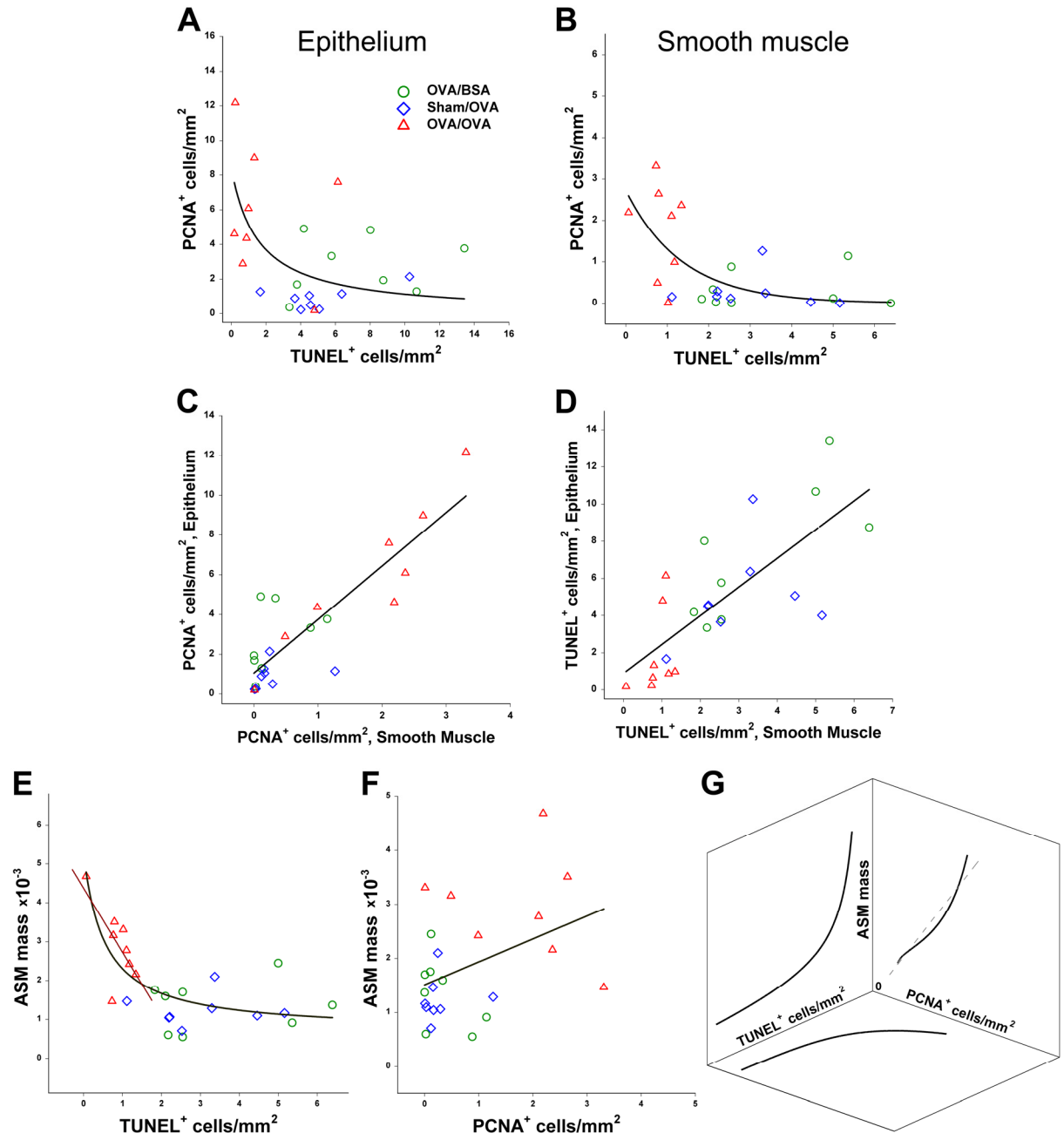
A
Epithelium
OVA/BSA
Sham/OVA
OVA/OVA
PCNA+ cells/mm2
TUNEL+ cells/mm2
B
Smooth muscle
PCNA+ cells/mm2
TUNEL+ cells/mm2
C
PCNA+ cells/mm2, Epithelium
PCNA+ cells/mm2, Smooth Muscle
D
TUNEL+ cells/mm2, Epithelium
TUNEL+ cells/mm2, Smooth Muscle
E
ASM mass x10-3
TUNEL+ cells/mm2
F
ASM mass x10-3
PCNA+ cells/mm2
G
ASM mass
TUNEL+ cells/mm2
PCNA+ cells/mm2